Pakistan Journal of Information and Technology 1(2): 118-125, 2002

Theoretical and Experimental Studies on a Thermosyphon Applied for Absorption Refrigerator Using LiBr-H_2O as Working Fluid

M. Mosa, Zhu Yuqun, Chen Jitao, A. Yattara, Chen Ying, Geng Wei and Zhang Jun
Refrigeration and Cryogenics Laboratory, Department of Power Engineering, Huazhong University of Science and Technology, Wuhan, China, 430074

Abstract: Based on the analysis of two-phase flow mechanism, transition from bubbly flow to slug flow and from slug flow to churn flow in a thermosyphon using LiBr- H_2O as working fluid have been modeled in this paper. Experiment has been setup to validate the theoretical model and to evaluate the pumping characteristics of the thermosyphon. The variations of the generator pressure, flow resistance and driving head with heat input are presented graphically. Results indicate that strong solution and vapor flow rates increase with heat input and so does the pumping ratio. In addition, the suitable heat input range corresponding to a certain thermosyphon tube diameter range was determined. These results can be used to design thermosyphons using LiBr-H_2O as working fluid.

Keywords: Flow Pattern, Thermosyphon, Water-Lithium Bromide, Absorption System

Introduction

Recently, refrigeration systems researches have been directed towards absorption type, this not only because of the environmental problems associated with utilization of conventional CFC's compression systems, but also the possibility of utilization of waste heat and solar energy for such systems. Since solution pump that conveys the solution from the absorber to the generator and creates the required pressure difference between condenser and evaporator requires a high-grade energy source, a fully heat-operated system stills a challenge. Thermosyphon in which vapor pressure generated acts as the driving force for conveying solution from the absorber to the generator is the promising system to replace this pump for application in a small capacity absorption refrigerator. Pumping characteristics of a thermosyphon applied for LiBr-H_2O system was investigated by Siyoung Jeong *et al.*. (1998). They made quantitative measurements of operating characteristics of the thermosyphon as a function of tube diameter, pumping height and heating power. Morcus Pfaff *et al.* (1998) investigated, both analytically and experimentally, the performance of a bubble pump for a LiBr-H_2O system. Their results indicate that pumping ratio is nearly independent of the heat pump input, but increases with decrease in pump tube diameter, decrease in pump lift and increase in driving head. With different operating conditions, i.e. liquid and gas flow rates, pipe diameter, entrance and exit conditions as well as physical properties four flow patterns may be observed in two-phase flow inside a vertical tube: mixed (bubbly) flow, slug flow, churn flow and annular flow (Mao, 1982). Since distribution characteristics and pressure drop of different flow pattern vary significantly, investigation in flow pattern analysis and transition regions becomes an important topic. With regard to water-lithium bromide vapor absorption refrigerator, the most important flow pattern is slug flow, therefore, in this paper theoretical and experimental investigation on the performance of a thermosyphon is made based on this type of flow pattern.

Theoretical Analysis of Flow Pattern

Transition from Bubbly Flow to Slug Flow: Investigations showed that in bubbly flow pattern sphere-like bubbles move upward when their diameters are small, but aberrance will take place, they will become hemispheres and go irregularly along spiral lines when their diameters exceed a critical value (Griffith and Wallis, 1961). When vapor mass flow increases to a certain level, the frequency of collisions among bubbles augments, and most bubbles join together forming bigger vapor bubbles which occupy almost the whole cross section of the tube when its diameter is small, thus the transition from bubbly flow to slug flow occurs. Griffith *et al.* (1961) and Radovich *et al.* (1962) deduced that the transition from bubbly flow to slug flow occurs at the void fraction around 0.3. Taitel *et al.* (1980) also proposed the same void fraction. Mishima *et al.* (1984) performed a simple analysis, which indicated that bubble flow would become unstable at a void fraction of 0.3. Also, according to some experimental data, when void fraction is less than 0.20 transition occur rarely and the fraction is seldom more than 0.3 (Chen *et al.*, 1983), (Chen *et al.*, 1992). Thus, the critical void fraction can be given by

$$\alpha_{tr} = 0.3 \quad (1)$$

If the vapour is considered as incompressible, the mass balance in bubbly flow yields:

$$U_{G}\alpha + U_{L}(1-\alpha) = U_{M} \quad (2)$$

where U_{G} and U_{L} are the actual phase velocities. U_{M} is

the mixture velocity given by

$$U_M = U_{SG} + U_{SL} \quad (3)$$

U_{SG} and U_{SL} are the superficial phase velocities given by

$$U_{SG} = U_G \alpha \quad (4)$$

$$U_{SL} = U_L (1-\alpha) \quad (5)$$

When the liquid velocity is relatively low the rising velocity of bubbles can be calculated by (Harmathy 1960):

$$U_B = 1.53\left[\frac{\sigma g(\rho_L - \rho_G)}{\rho_L^2}\right]^{\frac{1}{4}}(1-\alpha)^{1/2} \quad (6)$$

Hence,

$$U_G = U_L + 1.53\left[\frac{\sigma g(\rho_L - \rho_G)}{\rho_L^2}\right]^{\frac{1}{4}}(1-\alpha)^{1/2} \quad (7)$$

Using Eq. (2), (3), (4) and (5), Eq. (7) become:

$$\frac{U_{SG}}{U_{SL}} = \frac{\alpha}{1-\alpha} + 1.53\frac{\alpha(1-\alpha)^{1/2}}{U_{SL}}\left[\frac{\sigma g(\rho_L - \rho_G)}{\rho_L^2}\right]^{\frac{1}{4}} \quad (8)$$

Based on the critical condition, Eq. (1), the following equation is obtained:

$$U_{SL} = \frac{7}{3}U_{SG} - 0.9\left[\frac{\sigma g(\rho_L - \rho_G)}{\rho_L^2}\right]^{\frac{1}{4}} \quad (9)$$

Fig. 1 shows the transition from bubbly flow to slug flow map LiBr-H_2O solution in a thermosyphon. Thermodynamic properties of LiBr-H_2O solution and water are taken from (Dai and Zheng, 1980).

Transition from Slug Flow to Churn Flow: There are four factors affecting transition from slug flow to churn flow: entrance effect, wake stream effect, bubble forming effect and flooding effect. Because of their experimental base or unknown non-dimensional lengths, equations governing these factors are not convenient for application. Now, a new formula based on flooding

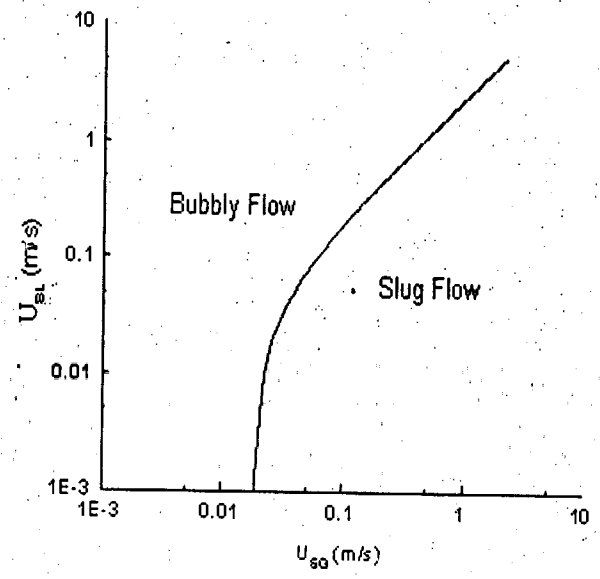

Fig. 1: Transition from Bubbly Flow to Slug Flow Map

phenomena can be developed.

In fully developed slug flow Taylor bubbles move upward steadily, whose diameters are as the same scale as the tube diameter. Between Taylor bubbles and tube's inner surface there is a liquid film flowing downward. When the vapor mass flow rate exceeds a critical value, the velocity of Taylor bubbles and the friction between downward-moving film and these bubbles increase sharply, so the film fluctuates up and down intermittently, thus flooding and transition to churn flow take place. Accordingly, critical conditions and governing equation can be deduced.

The continuity equation of Taylor bubbles region is given by:

$$U_{TB}\overline{\alpha} - (1-\overline{\alpha})U_F = U_M \quad (10)$$

When flooding occurs, the film becomes stagnant and the average film velocity:

$$U_F = 0 \quad (11)$$

Eq. (10) is reduced to:

$$U_{TB}\overline{\alpha} = U_M \quad (12)$$

Applying the force balance for gas core and liquid film, we obtain

$$-A_G\frac{dp}{dx} - \tau_i S_i - \rho_G A_G g = 0 \quad (13)$$

$$-A_L\frac{dp}{dx} + \tau_i S_i - \rho_L A_L g = 0 \quad (14)$$

Where τ_i is the interfacial shear stress, S_i is the interfacial periphary. A_G and A_L are flow cross-section areas of the liquid phase and the gas phase, respectively. $\frac{dp}{dx}$ is the pressure gradient along the flow direction..

Eliminating $\frac{dp}{dx}$ between Eq. (13) and Eq. (14) and substituting the following expressions

$A_L = A(1-\alpha)$ and $A_G = A\alpha$

into Eq. (13) and Eq. (14) gives

$$\tau_i S_i \left(\frac{1}{\alpha} + \frac{1}{1-\alpha} \right) = (\rho_L - \rho_G) g A \quad (15)$$

The interfacial shear stress is given by

$$\tau_i = f_i \frac{\rho_G (U_{TB} + U_L)^2}{2} \quad (16)$$

As $U_L = 0$, Eq. (16) become:

$$\tau_i = f_i \frac{\rho_G U_{TB}^2}{2} \quad (17)$$

U_{TB} is obtained as follows (Nicklin *et al.*, 1962):

$$U_{TB} = 1.2U_M + 0.35U_0 \quad (18)$$

Where

$$U_0 = \left[\frac{(\rho_L - \rho_G) g D}{\rho_L} \right]^{\frac{1}{2}} \quad (19)$$

The interfacial shear friction factor is given by (Bharathan *et al.*, 1979):

$$f_i = \left[1 + 12500 \left(1 - \alpha^{0.5} \right)^2 \right] C_G \left(\frac{U_M D}{\nu_G} \right)^{-m} \quad (20)$$

Where C_G and m are constants equal 0.0791 and 0.25, respectively and ν_G is the kinematics viscosity of the gas. Using Eq. (18), Eq. (17) become:

$$\tau_i = \left[1 + 12500 \left(1 - \alpha^{0.5} \right)^2 \right] C_G \left(\frac{U_M D}{\nu_G} \right)^{m} \frac{\rho_G U_{TB}^2}{2} \quad (21)$$

The interfacial periphery is given by

$$S_i = \pi D \alpha^{0.5} \quad (22)$$

And using Eq. (12), (18), (21) and (22), Eq. (15) become:

$$(1.2U_M + 0.35U_0)^{3.5} \times A = (0.2U_M + 0.35U_0) U_M^{0.75} \times B \quad (23)$$

Where,

$$A' = \frac{(\rho_L - \rho_G) g}{\frac{4C_G}{D} \left(\frac{DU_{SG}}{\nu_G} \right)^{-m} \frac{\rho_G U_{SG}^2}{2}} \quad (24)$$

$$B' = 1 + 12500 \left[1 - \left(\frac{U_M}{1.2U_M + 0.35U_0} \right)^{0.5} \right]^2 \quad (25)$$

Eq. (23) is the transition from slug flow to churn flow governing equation. Fig. 2 shows the transition from slug

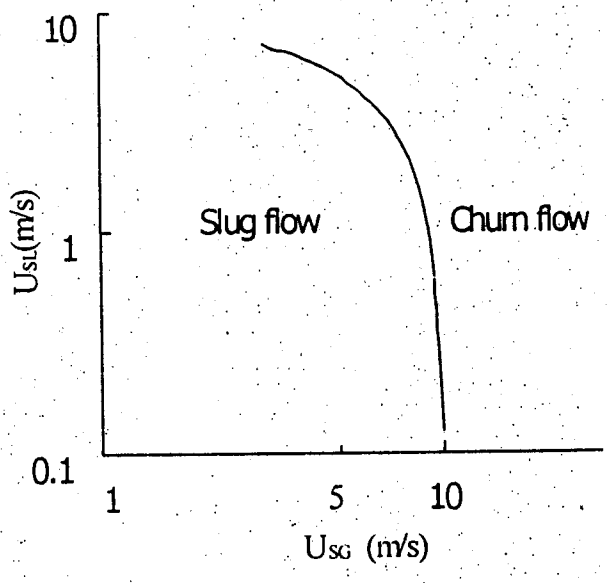

Fig. 2: Transition from Slug Flow to Churn Flow Map

flow to churn flow map of H_2O-LiBr two-phase flow in a thermosyphon.

Experimental Setup: The experimental setup is shown in Fig. 3. The main components are a generator, a thermosyphon (as a circulation pump), a separator, a

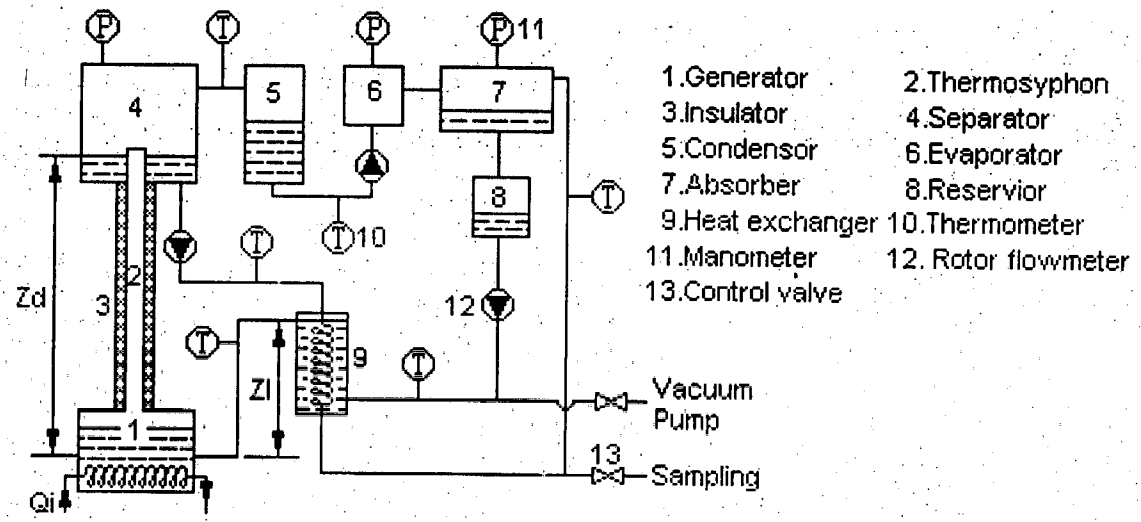

Fig. 3: Schematic Diagram of the Experimental Setup

condenser, an evaporator, a heat exchanger and appropriate instrumentation for measuring temperatures, pressures and flow rates. The tube diameter is (35 mm), pump lift (0.8 m), driving head (0.25 m) and pump heat input (3.3~5.3 kW). A vacuum pump is used to maintain the system at the desired vacuum pressure.

The test processes are as follows: The weak solution in the generator is first heated to saturation and then to the boiling point. The strong solution is then lifted to the separator by the thermosyphone. The vapor flows to the condenser where it liquefies and the solution flows through the heat exchanger back to the generator. The liquefied vapor is again evaporates in the evaporator, absorbed by LiBr-H_2O solution in the absorber and then flows back to the generator through the heat exchanger. Temperatures at various points were measured by T-type thermocouples. A mercury manometer is used to measure the pressure difference between the condenser and the generator (p_c-p_g). A gas burner is used as heat source. All readings are taken when steady state (which takes (5 ~ 10) minutes) is reached.

Results and Discussion

Analysis of Flow Patterns: According to correct judgment of flow patterns an effective experimental data and an accurate theoretical simulation results could be obtained. Fig. 4 shows experimentally the flow pattern map in the thermosyphon and it is slug as expected. In addition, from the governing equations, it can be seen that the essential factors influencing transition from bubbly flow to slug flow are not only the characteristic parameters of flow but also the superficial velocity. Tube diameter is also an important parameter that the critical superficial velocity of vapor increases as it increases.

Effect of Heat Input on Strong Solution and Vapor Flow Rates: The strong solution and vapor flow rates were measured with different heat inputs to investigate the performance of the thermosyphon. Fig. 5 shows, theoretically and experimentally, the strong solution flow rate variation with heat input. It can be seen that strong solution and vapor flow rates increase almost linearly with heat input but the experimental values are lower than the theoretical (ideal) ones.

Whally *et al.* (1983) have studied the relationship between strong solution flow rate and heat input and they suggested the following formula:

$$\dot{m}_L = \sqrt{Q_i (H_{fw} - H_{fr})} \qquad (26)$$

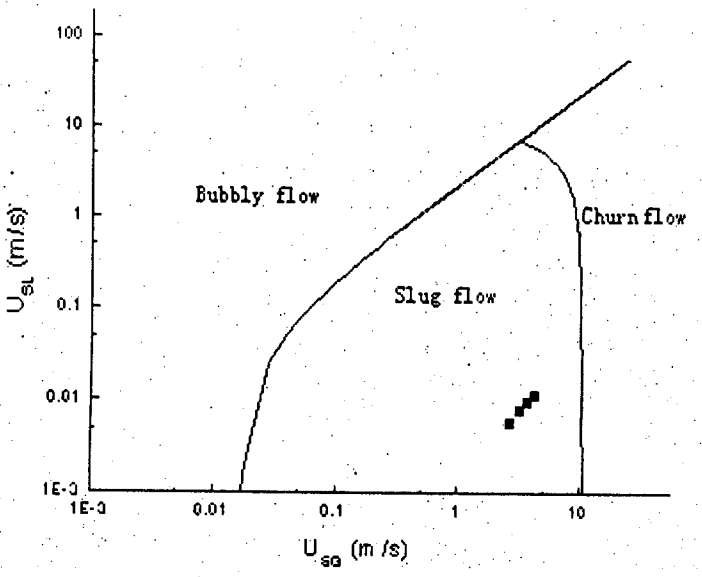

Fig. 4: Flow Pattern Map of Thermosyphon

Where $\dot{m}_l$ is the liquid flow rate and Q_i is the heat input. H_{th} and H_p are the theoretical and real driving

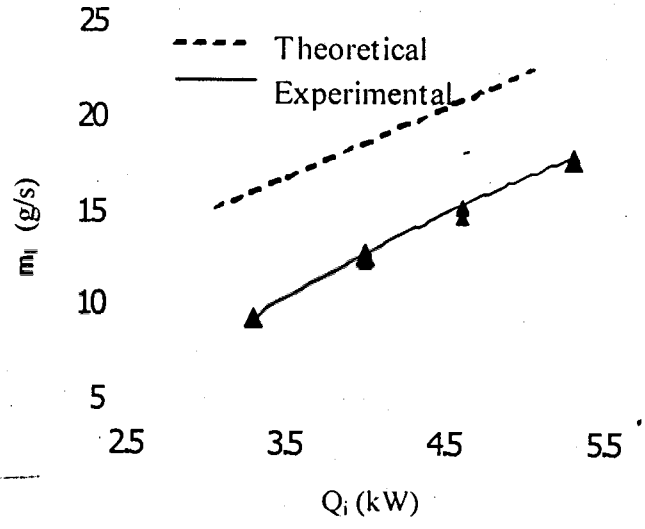

Fig. 5: Heat Input Effect on the Strong Solution Flow Rate

heads under certain heat input, respectively. Vapor flow rate is given by:

$$\dot{m}_v = \frac{Q_i}{h_s + fh_v} \quad (27)$$

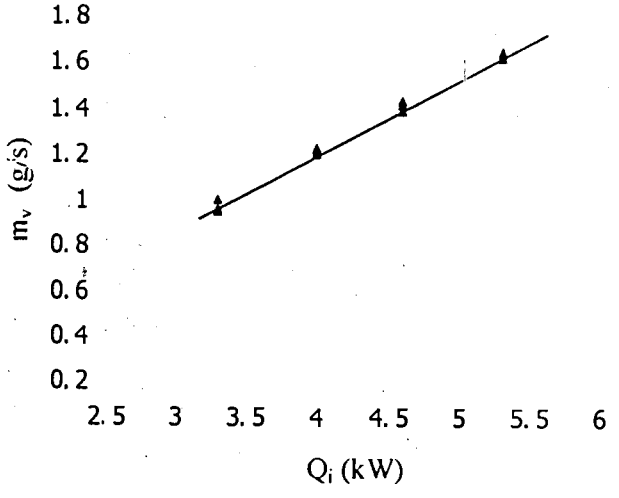

Fig. 6: Heat Input Effect on the Vapor Flow Rate

It can be seen that the refrigerant flow rate is determined by heat input (Q_i), latent heat of vaporization h_v, circulation ratio (f) and the sensible heat h_s. The latent heat of vaporization has greater influence on vapor flow rate than sensible heat with the same heat input, so the vapor flow rate shows a linear upward tendency for heat input, and the experimental results are in a good agreement as shown in Fig. 6.

Effect of Heat Input on the Pumping Ratio: Fig. 7

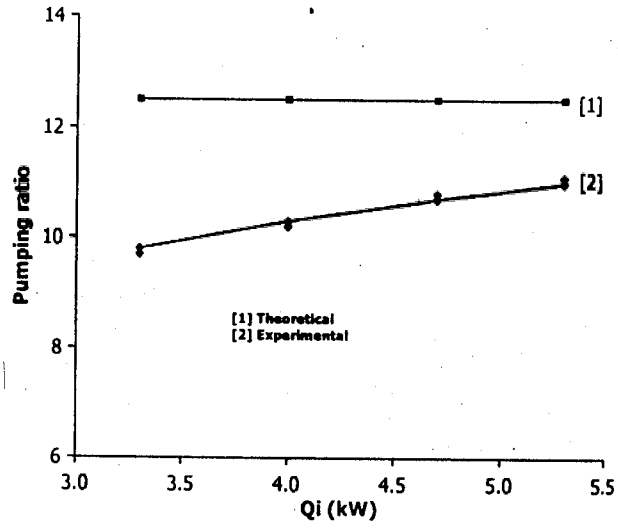

Fig. 7: Variation of Pumping Ratio with Heat Input

shows, theoretically and experimentally, the variation of the pumping ratio with heat inputs. It can be seen that pumping ratio increases with increasing heat input. This relationship can be explained as follows: When the weak solution was boiling in the generator, bubbles move upwards to the liquid surface and break into pieces, thus the liquid films wrapping the bubbles are torn into small drops and thrown into the vapor at the upper part of the generator. The height these drops can reach varies with drop size and the energy they gain from breaking up. Only those above the top of the vapor chamber can possibly be carried into the thermosyphon by the flowing vapor and then slug bubbles push them up into the liquid vapor separator. Those possessing higher energy have greater opportunity to be carried with increasing heat input. The latent heat of vaporization is much greater than liquid enthalpy difference, so the vapor flow rate is nearly constant. Pumping ratio is mainly determined by strong solution flow rate and the corresponding heat input. In addition, it can be seen that the theoretical pumping ratio is slightly greater than that of the experimental one. This difference could be explained as follows:

Theoretical pumping ratio is calculated using circulation ratio that conventionally applied to mechanical pumps and due to geometrical characteristics strong solution

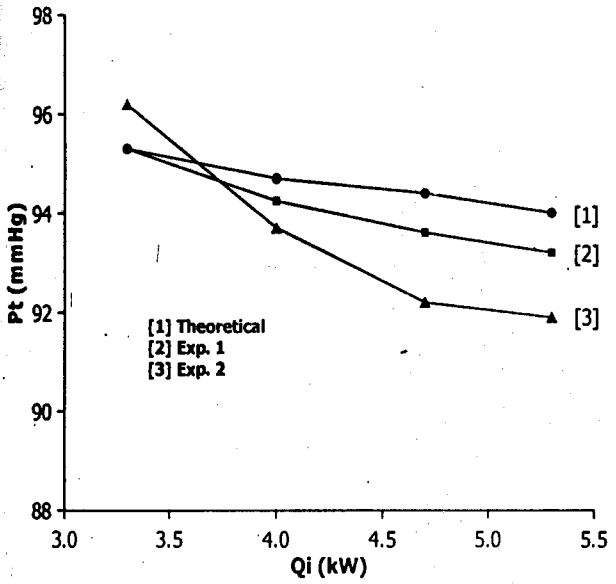

Fig. 8: Variation of Generator Pressure with Heat Input

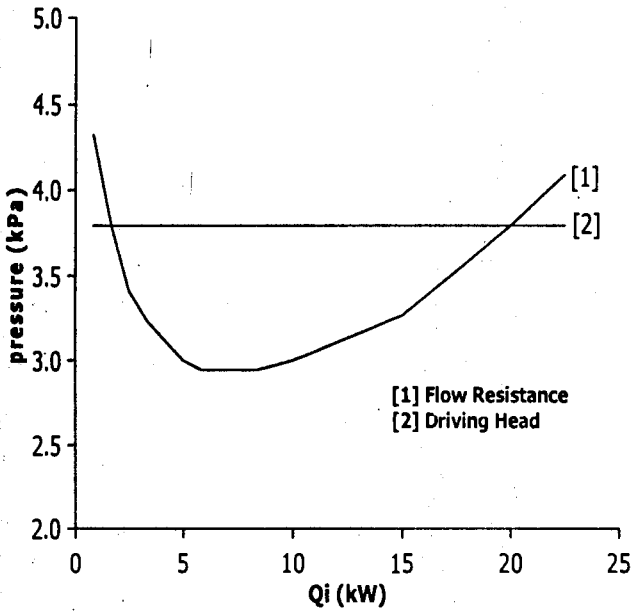

Fig. 9: Variation of Flow Resistance and Driving Head with Heat Input

can't be completely lifted to the separator and hence the actual pumping ratio is relatively lower.

Generator Pressure: The pressure in the generator is the sum of pressure in the condenser and pressure drop inside the thermosyphon. Fig. 8 shows its decreasing tendency with increasing heat input. It can be observed that the theoretical results are in a good agreement with the experimental ones.

Variation of Flow Resistance and Driving Head with Heat Input: The total flow resistance of the thermosyphon is composed of entrance resistance, two-phase flow pressure drop inside the tube and resistance to the weak solution flow. The experimental data also shows a downward tendency with increased heat input. The magnitude of driving head is determined by the merging height of the weak solution inside the reservoir which is kept constant throughout and so the driving head.

Theoretical analysis shows that the main part of the total flow resistance is the entrance resistance and the two-phase flow resistance and that of the weak solution is negligible as the flow rate is small. The larger the two-phase flow rate, the greater is the entrance resistance. Fig. 9 shows the theoretical variation of the total resistance with heat input. When the heat input is less than 7.1 kW, pressure drop of the tow-phase due to gravity is dominant and the total resistance decreases with increasing heat input. When a boundary value (7.1kW) is reached, the void fraction remains constant, whereas the entrance resistance and the weak solution flow resistance increase steadily with increasing heat input. Hence, a minimum resistance value exists for any tube diameter and according to it the refrigerator should be supplied with heat.

Heat Input Range: It can be seen from Fig. 9 that thermosyphon can operate with heat input range from 1.5 to 20.1 kW. However, according to the flow pattern transition curves shown in Fig. 4, it is found the minimum heat input required to take the flow pattern into slug flow is 0.016 kW, and when heat input exceeds 11.88 kW flow pattern will change to churn flow. Therefore, the reasonable range of heat input is 1.5 ~ 11.88 kW.

Tube Diameter Range: Researches have shown that a good thermosyphon performance will be obtained when flow is kept steadily slug. Under the conditions of fixed pump lift and driving head a range of diameters to keep the flow slug is obtained from the governing equations and the total pressure drop. Decreasing tube diameter causes velocity to increase, thus increases entrance resistance and friction pressure drop and finally causes the pump to stop working. Also, when the velocity exceeds a certain critical value the void fraction increases and flow pattern changes to churn flow, i.e., decreases strong solution flow rate and causes the pump to stop working due to crystallization in the generator. On the other hand, increasing diameter decreases the velocity and void fraction and increase mixture density and pressure drop due to gravity. Although the entrance resistance and the friction pressure drop will decrease, the total flow resistance will increase wholly, and when it exceeds driving head, the pump will stop working too. Variation of tube diameter range with heat input is shown in Table 1.

Table 1: Variation of Tube Diameter Range with Heat Input

Heat input (kW)	From driving head and total resistance		From slug flow governing equation		Optimum range	
	d_{max} (mm)	d_{min} (mm)	d_{max} (mm)	d_{min} (mm)	d_{max} (mm)	d_{min} (mm)
3.3	48.0	13.2	50.7	18.6	48.0	18.6
4.0	51.6	16.1	55.8	20.4	51.6	20.4
4.7	54.9	14.8	60.0	22.0	54.9	22.0
5.3	57.9	17.3	64.2	23.6	57.9	23.6

Nomenclature

A tube cross section area (m^2)
A_G gas flow cross section area (m^2)
A_L gas flow cross section area (m^2)
A', B' constants
C_G constant
D tube diameter (m)
f circulation factor
f_i interfacial shear friction factor
g acceleration due to gravity (m/s^2)
H_{tm} theoretical driving head (m)
H_p actual driving head (m)
h_s sensible heat (kJ/kg)
h_v latent heat of vaporization (kJ/kg)
m constant
m_L liquid flow rate (kg/m^3)
m_v vapor flow rate (kg/m^3)
P pressure (N/m^2)
Q_i heat input (kW)
S_i interfacial periphery (m)
U_F liquid film velocity (m/s)
U_G gas actual velocity (m/s)
U_L liquid actual velocity (m/s)
U_M mixture velocity (m/s)
U_o bubble rising velocity (m/s)
U_{SG} gas superficial velocity (m/s)
U_{SL} liquid superficial velocity (m/s)
U_{TB} Taylor bubble velocity (m/s)
α gas void fraction
α_c critical void fraction
$\overline{\alpha}$ average void fraction
σ surface tension (N/m)
ρ_G gas density (kg/m^3)
ρ_L liquid density (kg/m^3)
τ_i interfacial shear stress (N/m^2)
ν_G gas kinematic viscosity (m^2/s)

Acknowledgement
The Authors acknowledge the advice given by Prof. Zhu Yuqun during the course of this work.

Conclusion

Equations governing flow pattern transition in a thermosyphon using LiBr-H_2O solution as working fluid were modeled. A thermosyphon of 35 mm tube diameter, 0.8 m pump lift and 0.25 m driving head was built to validate the model. Pumping characteristics of the thermosyphon were investigated and the following conclusions were made.

- Governing equations of transition from bubbly to slug flow and from slug to churn flow were deduced based on analysis of two-phase flow mechanism and accordingly, flow pattern in the thermosyphon was distinguished.
- Pumping ratio, strong solution and vapor flow rate were measured, and rational explanation was given.
- The total flow pressure drop of the thermosyphon was measured and compared to the theoretical value. It was found that the suitable heat input range is 1.5 ~ 11.88 kW and thermosyphon tube diameter range with certain heat input was determined. The maximum suitable diameter range of the thermosyphon in this study is 48.0 ~ 57.9 mm and the minimum is 18.6 ~ 23.6 mm.

References

Bharathan D, G. B. Wallis, H. J. Richter, 1979. Air-water Counter-current Annular Flow in Vertical Tubes. Electric Power Research Institute Rep. EPRI NP-1165.

Chen Z, B. Cao , Z. Zhao, 1983. Gas Liquid Two-phase Flow and Heat Transfer. Mechanical Industry Publishing House, (in Chinese).

Chen X., X. Chen, F. Zhou, 1992. Mechanism and Criterion of Upward Gas Liquid Flow Pattern Transition. Transaction of Xian Jiaotong Uni. ;26 (in Chinese).

Dai Y, Y. Zheng, 1980. Absorption Refrigeration Machine. Mechanical Industry Publish House, (in Chinese).

Griffith P, G. B. Wallis, 1961. Two-phase Slug Flow. ASME, J. Heat Transfer; 83:307-320.

Harmathy T. Z., 1960. Velocity of Large Drops and Bubbles in Media of Infinite or Restricted Extent. AICHE J. 6:281-288.

Jorcus Pfaff, R. Saravanan, M. Prakash Maiya, S. Srinivasa, S. Murthy, 1998. Studies on Bubble Pump for Water-LiBr Vapor Absorption Refrigeration. Int J Refrigeration 21: 452-462.

Mao Y, G. Yu, 1982. Absorption and Vapor Ejector Refrigerator Mechanical Industry Publish House, (in Chinese).

Mishima K. M, M. Ishii, 1984. Flow Regime Transition Criteria for Upward Tow-phase Flow in Vertical Tubes. Int J. Heat and Mass Transfer: 27: 723-737.

Nicklin D. J, J. O. Wilkes, J. F. Davidson, 1962. Two-phase Flow in Vertical Tubes. Trans. Inst. Chem. Engrs; 40:61-68.

Radovich N. A, R. Moissis, 1962. The Transition from Two-phase Bubble Flow to Slug Flow. MIT Report. 7-7673-22.

Siyoung Jeong, Sang-Kyun Lee, 1998. Kee-Kahb Koo Pumping Characteristics of a Thermosyphon Applied for Absorption Refrigerators with Working Pair of LiBr/water. Applied Thermal Engineering 18:1309-1323.

Taitel Y, D. Bornea, A. E. Dukler, 1980. Modeling Flow Pattern Transitions for Steady Upward Gas-liquid Flow in Vertical Tubes. AICHE J. 26: 345-354.

Wally P. B, D. A. Butterworth, 1983. Simple Method of Calculating the Re-circulating Flow in Vertical Thermosyphon and Kettle Reboiler. 21st ASME, AICHE, National Heat Transfer Conference.